Two-Qubit State Tomography Using a Joint Dispersive Readout

S. Filipp,[1,*] P. Maurer,[1] P. J. Leek,[1] M. Baur,[1] R. Bianchetti,[1] J. M. Fink,[1] M. Göppl,[1] L. Steffen,[1] J. M. Gambetta,[2] A. Blais,[3] and A. Wallraff[1]

[1]*Department of Physics, ETH Zurich, CH-8093 Zurich, Switzerland*

[2]*Institute for Quantum Computing and Department of Physics and Astronomy, University of Waterloo, Waterloo, Ontario N2L 3G1, Canada*

[3]*Département de Physique, Université de Sherbrooke, Sherbrooke, Québec J1K 2R1, Canada*

(Received 17 December 2008; published 22 May 2009)

Quantum state tomography is an important tool in quantum information science for complete characterization of multiqubit states and their correlations. Here we report a method to perform a joint simultaneous readout of two superconducting qubits dispersively coupled to the same mode of a microwave transmission line resonator. The nonlinear dependence of the resonator transmission on the qubit state dependent cavity frequency allows us to extract the full two-qubit correlations without the need for single-shot readout of individual qubits. We employ standard tomographic techniques to reconstruct the density matrix of two-qubit quantum states.

DOI: 10.1103/PhysRevLett.102.200402 PACS numbers: 03.65.Wj, 03.67.Lx, 42.50.Pq, 85.35.Gv

Quantum state tomography allows for the reconstruction of an *a priori* unknown state of a quantum system by measuring a complete set of observables [1]. It is an essential tool in the development of quantum information processing [2] and has first been used to reconstruct the Wigner function [3] of a light mode [4] by homodyne measurements, as suggested in a seminal paper by Vogel and Risken [5]. Subsequently, state tomography has been applied to other systems with a continuous spectrum, for instance, to determine vibrational states of molecules [6], ions [7], and atoms [8]. Later, techniques have been adapted to systems with a discrete spectrum, for example, nuclear spins [9], polarization entangled photon pairs [10], electronic states of trapped ions [11], states of hybrid atom-photon systems [12], and spin-path entangled single neutrons [13].

Recent advances have enabled the coherent control of individual two-level systems embedded in a solid-state environment. Numerous experiments have been performed with superconducting quantum devices [14], manifesting the rapid progress and the promising future of this approach for quantum information processing. State tomographic methods [15] have been used to reconstruct density matrices of single qubits [16,17]. Even though a number of experiments showing coherent qubit-qubit interactions in superconducting circuits have already been performed [18–25], only a few have been able to reconstruct the full two-qubit density matrix. In fact, two-qubit states have been reconstructed by correlating high fidelity measurements obtained with individual qubit state detection [23]. Here we demonstrate the tomographic reconstruction of two-qubit states employing only a *single* measurement apparatus. In a superconducting circuit implementation of cavity quantum electrodynamics [26–28], we realize such a joint readout by measuring the transmission of a microwave frequency resonator strongly coupled to both qubits [24]. We are able to extract two-qubit correlations from an averaged measurement that acts simultaneously on the qubits. Instead of correlating measurement outcomes of individual qubit populations in each single-shot experiment, as routinely done [10–13,23], the averaged resonator response alone allows for full state tomography. This possibility has also been pointed out in [24].

In the setup shown in Fig. 1, two superconducting qubits are coupled to a transmission line resonator operating in the microwave regime [24]. Because of the large dipole moment of the qubits and the large vacuum field of the resonator, the strong coupling regime with $g_{1,2} \gg \kappa, \gamma_1$ is reached. $g_1/2\pi \approx g_2/2\pi = 133$ MHz denotes the similar coupling strengths of both qubits and $\kappa/2\pi \approx 1.7$ MHz and $\gamma_1/2\pi \approx 0.25$ MHz the photon and the qubit decay rates, respectively. The qubits are realized as transmons [29], a variant of a split Cooper pair box [30] with exponentially suppressed sensitivity to $1/f$ charge noise [31]. Their transition frequencies are tuned separately by external flux bias coils to $\omega_{a1}/2\pi = 4.5$ GHz and $\omega_{a2}/2\pi = 4.85$ GHz. Both qubits can be addressed individually through local gate lines using amplitude and phase modulated microwaves at frequencies ω_{d1} and ω_{d2}. Readout is accomplished by measuring the transmission of microwaves applied to the resonator input at frequency ω_m close to the fundamental resonator mode $\omega_r/2\pi = 6.442$ GHz.

At large detunings $\Delta_j \equiv \omega_r - \omega_{aj}$ of both qubits from the resonator, the dispersive qubit-resonator interaction gives rise to a qubit state dependent shift of the resonator frequency. In this dispersive limit and in a frame rotating at ω_m, the relevant Hamiltonian reads [32]

$$H = \hbar(\Delta_{rm} + \chi_1\hat{\sigma}_{z1} + \chi_2\hat{\sigma}_{z2})\hat{a}^\dagger\hat{a} + \frac{\hbar}{2}\sum_{j=1,2}(\omega_{aj} + \chi_j)\hat{\sigma}_{zj} + \hbar\epsilon(t)(\hat{a}^\dagger + \hat{a}), \quad (1)$$

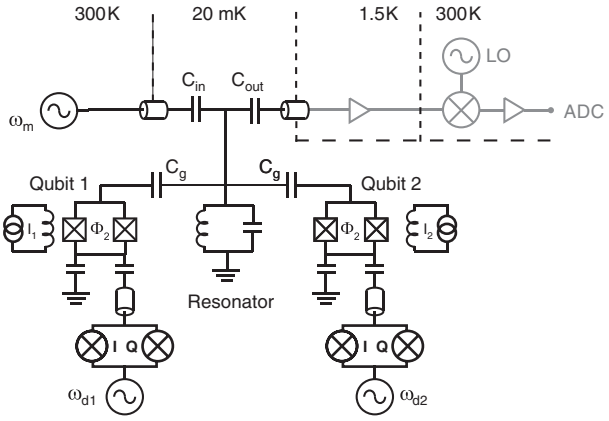

FIG. 1. Schematic of the experimental setup with two qubits coupled via the capacitances C_g to a microwave resonator operated at a temperature of about 20 mK. The transition frequencies of the qubits are adjusted by external fluxes Φ_1 and Φ_2. The resonator-qubit system is probed through the input and output capacitances $C_{\rm in}$ and $C_{\rm out}$, respectively, by a microwave signal at frequency ω_m. Additionally, local control of the qubits is implemented by capacitively coupled signals ω_{d1} and ω_{d2}, which are phase and amplitude modulated using in-phase/quadrature (I/Q) mixers. The output signal is detected in a homodyne measurement at room temperature.

where $\Delta_{rm} \equiv \omega_r - \omega_m$ is the detuning of the measurement drive from the resonator frequency. The cavity pulls $\chi_1 = -1$ MHz and $\chi_2 = -1.5$ MHz are determined by the detuning $\Delta_{1,2}$, the coupling strength $g_{1,2}$, and the design parameters of the qubit [29]. The last term in Eq. (1) models the measurement drive with amplitude $\epsilon(t)$.

The operator $\hat{\chi} \equiv \chi_1\hat{\sigma}_{z1} + \chi_2\hat{\sigma}_{z2}$, which describes the dispersive shift of the resonator frequency, is linear in both qubit states. It does not contain two-qubit terms like $\hat{\sigma}_{z1}\hat{\sigma}_{z2}$ from which information about the qubit-qubit correlations could be obtained. However, in circuit QED, instead of measuring frequency shifts directly, we record quadrature amplitudes of microwave transmission through the resonator which depend nonlinearly on these shifts. The average values of the field quadratures $\langle\hat{I}(t)\rangle = [\hat{\rho}(t)(\hat{a}^\dagger + \hat{a})]$ and $\langle\hat{Q}(t)\rangle = i\,\mathrm{Tr}[\hat{\rho}(t)(\hat{a}^\dagger - \hat{a})]$ are determined from the amplified voltage signal at the resonator output in a homodyne measurement, where $\hat{\rho}(t)$ denotes the state of both qubits and resonator field.

These expressions can be evaluated by assuming an initially separable state $\hat{\rho}(0) = |0\rangle\langle 0| \otimes \hat{\rho}_q(0)$ for the qubits $[\hat{\rho}_q(0)]$ and the resonator $[|0\rangle\langle 0|]$. Taking $\hat{\rho}_q(0) = \sum_{\sigma,\sigma'} p_{\sigma\sigma'}(0)|\sigma\rangle\langle\sigma'|$, with $\sigma = \{ee, eg, ge, gg\}$, the combined qubits-resonator state at time t under Eq. (1) and cavity damping can be expressed as $\hat{\rho}(t) = \sum_{\sigma,\sigma'} p_{\sigma\sigma'}(t)|\sigma\alpha_\sigma\rangle\langle\sigma'\alpha_{\sigma'}|$ [33]. In this expression, α_σ is the coherent state amplitude given that the qubits are in state $|\sigma\rangle$ and satisfies $\dot{\alpha}_\sigma = -i(\Delta_{rm} + \langle\sigma|\hat{\chi}|\sigma\rangle)\alpha_\sigma - i\epsilon - \kappa\alpha_\sigma/2$. Since this is a quantum nondemolition measurement [27], $p_{\sigma\sigma}(t) = p_{\sigma\sigma}(0)$, and the off-diagonal terms $p_{\sigma\sigma'}(t)$ contain an ac-Stark shift and dephasing, both induced by the measurement.

Taking the trace on the resonator space yields $\langle\hat{I}(t)\rangle, \langle\hat{Q}(t)\rangle = \mathrm{Tr}_q[\hat{\rho}_q(0)\hat{M}_{I,Q}(t)]$, where $\hat{M}_{I,Q}(t) = \sum_\sigma\langle\alpha_\sigma(t)|\hat{I}, \hat{Q}|\alpha_\sigma(t)\rangle|\sigma\rangle\langle\sigma|$ and Tr_q denotes the partial trace over the qubits. In the steady state we find

$$\hat{M}_I = -\epsilon\frac{2(\Delta_{rm} + \hat{\chi})}{(\Delta_{rm} + \hat{\chi})^2 + (\kappa/2)^2}, \tag{2}$$

$$\hat{M}_Q = -\epsilon\frac{\kappa}{(\Delta_{rm} + \hat{\chi})^2 + (\kappa/2)^2}, \tag{3}$$

demonstrating that the measurement operators are nonlinear functions of $\hat{\chi}$. Thus, $\hat{M}_{I,Q}$ comprises in general also two-qubit correlation terms proportional to $\hat{\sigma}_{z1}\hat{\sigma}_{z2}$, which allow one to reconstruct the full two-qubit state.

In our experiments the phase of the measurement microwave at frequency $\Delta_{rm} = (\chi_1 + \chi_2)$ is adjusted such that the Q quadrature of the transmitted signal carries most of the signal when both qubits are in the ground state. The corresponding measurement operator can be expressed as

$$\hat{M} = \tfrac{1}{4}(\beta_{00}\hat{\mathrm{id}} + \beta_{10}\hat{\sigma}_{z1} + \beta_{01}\hat{\sigma}_{z2} + \beta_{11}\hat{\sigma}_{z1}\hat{\sigma}_{z2}), \tag{4}$$

with $\beta_{ij} = \alpha_{--} + (-1)^j\alpha_{-+} + (-1)^i\alpha_{+-} + (-1)^{i+j}\alpha_{++}$ and

$$\alpha_{\pm\pm} = -\kappa\{(\kappa/2)^2 + (\Delta_{rm} \pm \chi_1 \pm \chi_2)^2\}^{-1/2} \tag{5}$$

representing the qubit state dependent Q-quadrature amplitudes of the resonator field in the steady-state limit and for an infinite qubit lifetime [Fig. 2(a)].

Since we operate in a regime where the qubit relaxation cannot be neglected, the steady-state expression is of lim-

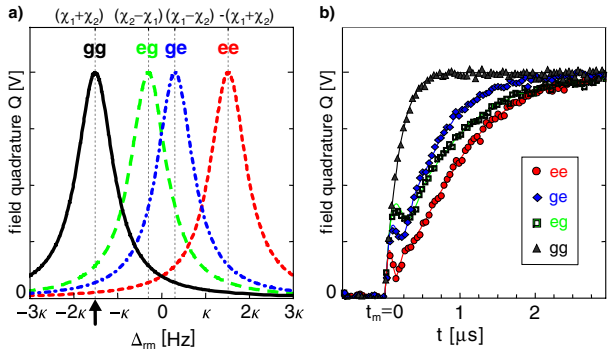

FIG. 2 (color online). (a) Q quadrature of the resonator field for the qubits in states gg, eg, ge, and ee as a function of the detuning Δ_{rm}. Tomography measurements have been performed at $\Delta_{rm} = (\chi_1 + \chi_2)$ indicated by an arrow. (b) Measured (data points) time evolution of the Q quadrature for the indicated initial states compared to numerically calculated responses (solid lines). All parameters have been determined in independent measurements.

ited practical use. The decay of a qubit to its ground state changes the resonance frequency of the resonator and consequently limits the readout time to $\sim 1/\gamma_1$. A typical averaged time trace of the resonator response for pulsed measurements is shown in Fig. 2(b), similar to the data presented in Ref. [24]. The qubits are prepared initially in the states $|ee\rangle$, $|eg\rangle$, $|ge\rangle$, and $|gg\rangle$, respectively, using the local gate lines. The time dependence of the measurement signal is determined by the rise time of the resonator and the decay time of the qubits. It is in excellent agreement with calculations [solid lines in Fig. 2(b)] of the dynamics of the dispersive Jaynes-Cummings Hamiltonian [32,34] using the parameter values as stated above. Because of the quantum nondemolition nature of the measurement [27], $\hat{M}$ remains diagonal in the instantaneous qubit eigenbasis during the measurement process, and the integrated signal can be used to define the realistic measurement operator $\hat{M}'$ by replacing the $\alpha_{\pm\pm}$ in Eq. (5) with the signal integrated from the start of the measurement t_m to the final time T, $\alpha'_{\pm\pm} = 1/N \int_{t_m}^{T} [\langle \hat{M}(t)\rangle_{\pm\pm} - \langle \hat{M}(t)\rangle_{--}]dt$ with the ground state response $\langle \hat{M}(t)\rangle_{--}$ subtracted. The normalization constant N is chosen such that $\alpha'_{+-} = 1$ and the measurement time $T - t_m = 2\ \mu$s.

To reconstruct the combined state $\hat{\rho}_q$ of both qubits, a suitable set of measurements has to be found to determine unambiguously the 16 coefficients r_{ij} of the density matrix $\hat{\rho}_q = \sum_{i,j=0}^{3} r_{ij} \hat{\sigma}_i \otimes \hat{\sigma}_j$, with the identity $\hat{\sigma}_0 = \hat{\mathrm{id}}$ and $\{\hat{\sigma}_1, \hat{\sigma}_2, \hat{\sigma}_3\} = \{\hat{\sigma}_x, \hat{\sigma}_y, \hat{\sigma}_z\}$. Such a complete set of measurements is constructed by applying appropriate single-qubit rotations $\hat{U}_k \in SU(2) \otimes SU(2)$ before the measurement in order to measure the expectation values $\langle \hat{M}_k \rangle = \mathrm{Tr}[\hat{M}\hat{U}_k \hat{\rho}_q \hat{U}_k^\dagger] = \mathrm{Tr}[\hat{U}_k^\dagger \hat{M} \hat{U}_k \hat{\rho}_q]$. The latter equality defines the set of measurement operators $\hat{M}_k \equiv \hat{U}_k^\dagger \hat{M} \hat{U}_k$. This illustrates again that a measurement operator $\hat{M}$ involving nontrivial two-qubit terms $\hat{\sigma}_{i1}\hat{\sigma}_{j2}$ is necessary for state tomography. In fact, single-qubit operations $\hat{U}_k = \hat{U}_{k1} \otimes \hat{U}_{k2}$ alone cannot be used to generate correlation terms since $\hat{U}_k^\dagger(\hat{\mathrm{id}} \otimes \hat{\sigma}_z)\hat{U}_k = \hat{\mathrm{id}} \otimes (\hat{U}_{k2}^\dagger \hat{\sigma}_z \hat{U}_{k2})$, for instance. As $\mathrm{Tr}[(\hat{\sigma}_k \otimes \hat{\sigma}_l)(\hat{\sigma}_m \otimes \hat{\sigma}_n)] = \delta_{km}\delta_{ln}$, some coefficients r_{ij} of the density matrix $\hat{\rho}_q$ would not be determined in an averaged measurement.

To identify the coefficients r_{ij} we perform 16 linearly independent measurements. The condition for the completeness of the set of tomographic measurements is the nonsingularity of the matrix A defined by the relation $\langle \hat{M}_k \rangle = \sum_{l=0}^{15} A_{kl} r_l$ between the expectation values $\langle \hat{M}_k \rangle$ and the coefficients of the density matrix r_l with $l \equiv i + 4j$. Our pulse scheme for the state tomography is shown in Fig. 3. First, a given two-qubit state is prepared. Then a complete set of measurements is formed by applying the combination of $\{(\pi/2)_x, (\pi/2)_y, (\pi), \mathrm{id}\}$ pulses to both qubits over their individual gate lines using amplitude and phase controlled microwave signals. The desired rotation

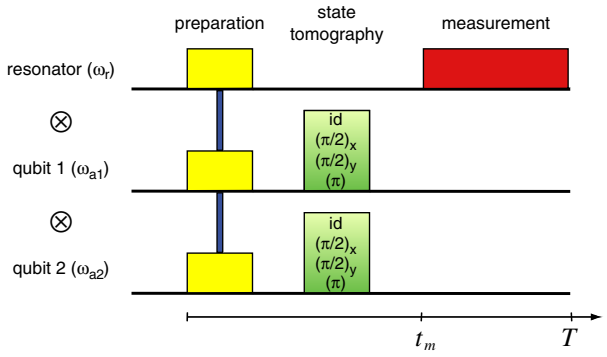

FIG. 3 (color online). Pulse scheme for tomography; see text.

angles are realized with an accuracy better than 4°. Finally, the measurement drive is applied at $\omega_m = 6.445$ GHz corresponding to the maximum transmission frequency of the resonator with both qubits in the ground state.

To determine the measurement operator $\hat{M}'$, π pulses are alternately applied to both qubits to yield signals as shown in Fig. 2(b). From these data the coefficients $(\beta'_{00}, \beta'_{01}, \beta'_{10}, \beta'_{11}) = (0.8, -0.3, -0.4, -0.1)$ of $\hat{M}'$ in Eq. (4) are deduced. The nonvanishing β'_{11}, which quantifies the contribution of the $\hat{\sigma}_z \otimes \hat{\sigma}_z$ two-qubit correlation term, allows for a measurement of arbitrary, entangled and separable, quantum states. As an example of this state reconstruction, in Fig. 4(a) the extracted density matrix $\hat{\rho}_q$ of the product state $|\Psi_{\mathrm{sep}}\rangle = 1/\sqrt{2}(|g\rangle + |e\rangle) \otimes 1/\sqrt{2}(|g\rangle + i|e\rangle)$ is shown. Using sideband transitions [32,35], the Bell state $|\Phi\rangle = 1/\sqrt{2}(|g\rangle \otimes |g\rangle - i|e\rangle \otimes |e\rangle)$ has been prepared by a sequence of pulses on the blue sidebands of both qubits [36]. Its reconstructed density matrix is shown in Fig. 4(b). 6.6×10^4 and 6.6×10^5 records have been averaged, respectively, for each of the 16 tomographic measurement pulses to determine the expectation values $\langle \hat{M}'_k \rangle$ for the two states. The corresponding ideal state tomograms are depicted in Figs. 4(c) and 4(d). To avoid unphysical, non-positive-semidefinite, density matrices originating from statistical uncertainties, all tomography data have been processed by a maximum likelihood method [37,38]. The corresponding fidelities $\mathcal{F}_\psi \equiv \langle \psi | \hat{\rho}_q | \psi \rangle^{1/2}$ are $\mathcal{F}_{\mathrm{sep}} = 95\%$ and $\mathcal{F}_{\Phi^-} = 74\%$. These results are in close agreement with theoretically expected fidelities when taking finite photon and qubit lifetimes into account. In particular, the loss in fidelity of the Bell state is not due to measurement errors but due to the short photon lifetime [36]. Note that our method has also been successfully applied to perform readout in a circuit QED implementation of quantum algorithms [39].

In conclusion, we have presented a method to jointly and simultaneously read out the quantum state of two qubits dispersively coupled to a microwave resonator. In a measurement of the field quadrature amplitudes of microwaves transmitted through the resonator, each photon carries

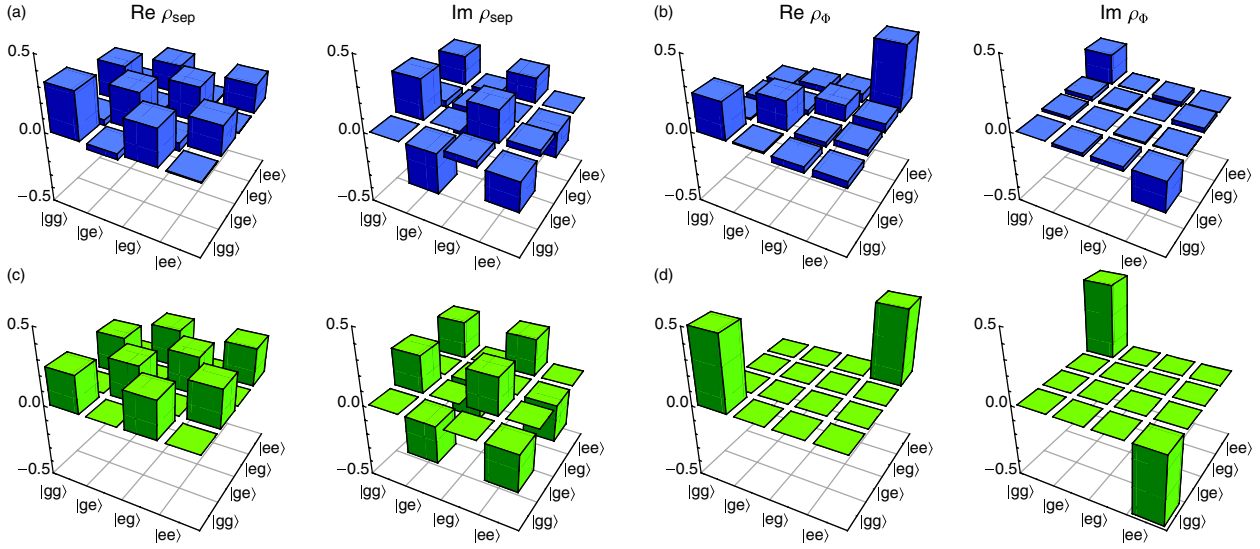

FIG. 4 (color online). Real and imaginary parts of reconstructed density matrices of (a) the product state $|\Psi_{sep}\rangle = 1/\sqrt{2}(|g\rangle + |e\rangle) \otimes 1/\sqrt{2}(|g\rangle + i|e\rangle)$ and (b) the Bell state $|\Phi\rangle = 1/\sqrt{2}(|g\rangle \otimes |g\rangle - i|e\rangle \otimes |e\rangle)$. Ideal tomograms are shown in (c) and (d).

information about the state of both qubits. In this way the two-qubit correlations can be extracted from an averaged measurement of the transmission amplitude without the need for single-shot and single-qubit readout, which enables the reconstruction of any correlated two-qubit state from a quantum nondemolition measurement. This method can also be extended to multiple qubits coupled to the same resonator mode.

We acknowledge the group of M. Siegel at the University of Karlsruhe for the preparation of niobium films. This work was supported by Swiss National Science Foundation (SNF) and ETH Zurich. P. J. L. was supported by the EC with a MC-EIF, J. M. G. by CIFAR, MRI, MITACS, and NSERC, and A. B. by NSERC and CIFAR.

*filipp@phys.ethz.ch

[1] *Quantum State Estimation*, edited by M. Paris and J. Řeháček (Springer, Berlin, 2004).
[2] M. A. Nielsen and I. L. Chuang, *Quantum Computation and Quantum Information* (Cambridge University Press, Cambridge, England, 2000).
[3] W. Schleich, *Quantum Optics in Phase Space* (Wiley-VCH, Berlin, 2001).
[4] D. T. Smithey, M. Beck, M. G. Raymer, and A. Faridani, Phys. Rev. Lett. **70**, 1244 (1993).
[5] K. Vogel and H. Risken, Phys. Rev. A **40**, 2847 (1989).
[6] T. J. Dunn, I. A. Walmsley, and S. Mukamel, Phys. Rev. Lett. **74**, 884 (1995).
[7] D. Leibfried *et al.*, Phys. Rev. Lett. **77**, 4281 (1996).
[8] C. Kurtsiefer, T. Pfau, and J. Mlynek, Nature (London) **386**, 150 (1997).
[9] I. L. Chuang *et al.*, Nature (London) **393**, 143 (1998).
[10] A. G. White, D. F. V. James, P. H. Eberhard, and P. G. Kwiat, Phys. Rev. Lett. **83**, 3103 (1999).
[11] C. F. Roos *et al.*, Science **304**, 1478 (2004).
[12] J. Volz *et al.*, Phys. Rev. Lett. **96**, 030404 (2006).
[13] Y. Hasegawa *et al.*, Phys. Rev. A **76**, 052108 (2007).
[14] J. Clarke and F. K. Wilhelm, Nature (London) **453**, 1031 (2008).
[15] Yu-xi Liu, L. F. Wei, and F. Nori, Phys. Rev. B **72**, 014547 (2005).
[16] M. Steffen *et al.*, Phys. Rev. Lett. **97**, 050502 (2006).
[17] A. A. Houck *et al.*, Nature (London) **449**, 328 (2007).
[18] Yu. A. Pashkin *et al.*, Nature (London) **421**, 823 (2003).
[19] T. Yamamoto *et al.*, Nature (London) **425**, 941 (2003).
[20] R. McDermott *et al.*, Science **307**, 1299 (2005).
[21] A. O. Niskanen *et al.*, Science **316**, 723 (2007).
[22] J. H. Plantenberg *et al.*, Nature (London) **447**, 836 (2007).
[23] M. Steffen *et al.*, Science **313**, 1423 (2006).
[24] J. Majer *et al.*, Nature (London) **449**, 443 (2007).
[25] M. A. Sillanpää *et al.*, Nature (London) **449**, 438 (2007).
[26] A. Wallraff *et al.*, Nature (London) **431**, 162 (2004).
[27] A. Blais *et al.*, Phys. Rev. A **69**, 062320 (2004).
[28] R. Schoelkopf and S. Girvin, Nature (London) **451**, 664 (2008).
[29] J. Koch *et al.*, Phys. Rev. A **76**, 042319 (2007).
[30] V. Bouchiat *et al.*, Phys. Scr. **T76**, 165 (1998).
[31] J. A. Schreier *et al.*, Phys. Rev. B **77**, 180502(R) (2008).
[32] A. Blais *et al.*, Phys. Rev. A **75**, 032329 (2007).
[33] J. Gambetta *et al.*, Phys. Rev. A **77**, 012112 (2008).
[34] R. Bianchetti *et al.* (to be published).
[35] A. Wallraff *et al.*, Phys. Rev. Lett. **99**, 050501 (2007).
[36] P. J. Leek *et al.*, arXiv:0812.2678 [Phys. Rev. B (to be published)].
[37] Z. Hradil, Phys. Rev. A **55**, R1561 (1997).
[38] D. F. V. James, P. G. Kwiat, W. J. Munro, and A. G. White, Phys. Rev. A **64**, 052312 (2001).
[39] L. DiCarlo *et al.*, arXiv:0903.2030.